Biochimica et Biophysica Acta 1803 (2010) 1154–1163

Contents lists available at ScienceDirect

Biochimica et Biophysica Acta

journal homepage: www.elsevier.com/locate/bbamcr

Absence of ataxin-3 leads to cytoskeletal disorganization and increased cell death

Ana-João Rodrigues [a,1], Maria do Carmo Costa [a,b,1], Teresa-Luísa Silva [a], Daniela Ferreira [a], Fernanda Bajanca [a,2], Elsa Logarinho [a,c], Patrícia Maciel [a,*]

[a] Life and Health Sciences Research Institute (ICVS), School of Health Sciences, University of Minho, Braga, Portugal
[b] Department of Neurology, University of Michigan, Ann Arbor, USA
[c] Institute for Molecular and Cell Biology (IBMC), Porto, Portugal

ARTICLE INFO

Article history:
Received 6 January 2010
Received in revised form 3 May 2010
Accepted 8 July 2010
Available online 15 July 2010

Keywords:
Polyglutamine
Ubiquitin–proteasome
Sinocerebellar ataxia type 3
Tubulin

ABSTRACT

Ataxin-3 (ATXN3) is a widely expressed protein that binds to ubiquitylated proteins, has deubiquitylating activity *in vitro* and is thought to modulate substrate degradation through the ubiquitin–proteasome pathway. Expansion of a polyglutamine tract in ATXN3 causes Machado–Joseph disease, a late-onset neurodegenerative disorder characterized by ubiquitin-positive aggregate formation and specific neuronal death. Although ATXN3 has been involved in transcriptional repression and in the ubiquitin–proteasome pathway, its biological function is still unknown.

In this work, we show that depletion of ATXN3 using small-interference RNA (siRNA) causes a prominent phenotype in both human and mouse cell lines. A mild increase in ubiquitylation occurs and cells exhibit ubiquitin-positive foci, which is consistent with ATXN3 putative function as a deubiquitylating enzyme. In addition, siATXN3-silenced cells exhibit marked morphological changes such as rounder shape and loss of adhesion protrusions. At a structural level, the microtubule, microfilament and intermediate filament networks are severely compromised and disorganized. This cytoskeletal phenotype is reversible and dependent on ATXN3 levels. Cell–extracellular matrix connection is also affected in ATXN3-depleted cells as talin expression is reduced in the focal adhesions and lower levels of α-1 integrin subunit are expressed at their surface. Although the cytoskeletal and adhesion problems do not originate any major change in the cell cycle of siATXN3-depleted cells, cell death is increased in siATXN3 cultures compared to controls.

In summary, in this work we show that the absence of ATXN3 leads to an overt cytoskeletal/adhesion defect raising the possibility that this protein may play a role in the cytoskeleton.

1. Introduction

Ataxin-3 (ATXN3) is the protein involved in Machado–Joseph Disease (MJD), also known as Spinocerebellar Ataxia Type 3 (SCA3), a late onset neurodegenerative disorder that belongs to the group of polyglutamine (polyQ) diseases [1].

ATXN3 possesses a josephin domain (JD) and, depending on the isoform, two or three ubiquitin interacting motifs (UIMs). ATXN3 has been involved in the ubiquitin–proteasome pathway (UPP) considering that (i) it interacts with ubiquitin, polyubiquitin chains, ubiquitin-like protein Nedd8 and with ubiquitylated proteins [2–5]; (ii) it has deubiquitylating (DUB) activity *in vitro* mediated by the JD domain being able to bind and cleave K48 polyubiquitin chains [2,3,6] which are a common recognition motif for proteasomal degradation; iii) it interacts with subunits of the proteasome [2,7] and iv) with VCP/p97, known to be involved in the shuttling of substrates for proteasomal degradation [8,9].

Besides cleaving K48 polyubiquitin chains, ATXN3 also has DUB activity against K63 chains and mixed linkage chains [10], which suggests that ATXN3 can be involved in other cellular processes dependent on K63 linkage such as DNA repair, transcriptional regulation, endocytosis and activation of protein kinases [11]. In addition to its role as a DUB, ATXN3 was proposed to repress transcription by directly binding to chromatin, inhibiting histone acetylation and by recruiting repressor complexes [12,13].

The cytoskeleton is a heterogeneous network of filamentous structures, composed of microfilaments, intermediate filaments, and microtubules. Neurons are particularly dependent on the cytoskeleton to deliver the proteins synthesized in the cell body to the axons and nerve terminals. Therefore, dysfunction of cytoskeletal components has been proposed as a feature of several neurodegenerative diseases including Alzheimer´s disease (AD), tauopathies and polyQ disorders [14,15]. For example, AD is characterized by the formation of insoluble neurofibrillary tangles (NFT) that contain tau protein, a microtubule

* Corresponding author. Life and Health Sciences Research Institute (ICVS), School of Health Sciences, University of Minho, 4710-057 Braga, Portugal. Fax: +351 253 604 820.
E-mail address: pmaciel@ecsaude.uminho.pt (P. Maciel).
[1] These authors contributed equally to this work.
[2] Present address: Randall Division for Cell and Molecular Biophysics, King's College London, UK.

0167-4889/$ – see front matter © 2010 Elsevier B.V. All rights reserved.
doi:10.1016/j.bbamcr.2010.07.004

binding protein that stabilizes the microtubule tracts necessary for vesicular trafficking, endo- and exocytosis and axonal polarity. Tau in NFT is typically hyperphosphorylated and, in this state, tubulin assembly is impaired [16]. Huntingtin (htt), a polyQ protein involved in Huntington's disease, co-fractionates with microtubules *in vitro*, interacts with β-tubulin and associates with the HAP1 protein, a partner of dynactin p150Glued, a component of the cytoplasmic dynein motor responsible for microtubule-dependent retrograde transport [17,18].

When the cellular chaperones and UPP are both compromised or overwhelmed, misfolded proteins are transported to form aggresomes, which are located in the perinuclear area near the microtubule-organizing center [19]. Microtubules are involved in aggresome formation as well as the motor proteins dynein and dynactin and the microtubule-associated protein histone deacetylase 6 (HDAC6) [20,21]. Interestingly, it has been described that ATXN3 interacts with dynein and HDAC6, its DUB activity and the ubiquitin-binding properties of its UIMs being required for aggresome formation [8,22], although the exact role of ATXN3 in this mechanism remains unclear.

Our previous findings showing that mouse ATXN3 is highly expressed in all types of muscle, in ciliated cells and in the flagellum of spermatozoids [23], and that several transcripts related to structure/motility were altered in the *Caenorhabditis elegans atx-3* knockout animals [24], suggested a possible link between ATXN3 and the cytoskeleton. In fact, recent data has shown that tubulin interacts with ATXN3, although the functional relevance of this interaction was not clarified [8,25].

In this study we used RNA interference-mediated ATXN3 knockdown to study the cellular role of this protein; we show that lack of ATXN3 leads to a marked cellular phenotype in both human and mouse cell lines. Besides accumulating ubiquitylated material in small foci in the cytoplasm, the ATXN-3-depleted cells are rounder, display less projections and present evident cytoskeletal disorganization, loss of cell adhesion and increased cell death.

2. Materials and methods

2.1. RNA interference

Gene regions of human *ATXN3* gene (nucleotides 113–826 from the start codon; NM_004993) and mouse m*ATXN3* gene (the first 646 nucleotides from the start codon; NM_029705), predicted to contain efficient siRNA target sequences (BLOCKiT RNAi design tool, Invitrogen) were amplified with primers RNAi_hATXN3F + RNAi_hATXN3R and mmMJD106 + mmMJD10, respectively, using standard procedures (Sup. Table 1). The PCR products were then transcribed using the BLOCK-iT TOPO Transcription Kit (Invitrogen). Diced siRNA pools were generated from dsRNA using the BLOCK-iT™ Dicer RNAi Transfection Kit accordingly to manufacturer's instructions (Invitrogen). Control siRNA was synthesized using the same protocol. The primers used for the amplification of UBXD8 (control RNAi) were RNAi_UBXD8F and RNAi_UBXD8R (Sup. Table 1). This gene was used as a control as it is also involved in the UPP.

2.2. Cell culture and transfection

HeLa cells were purchased from ATCC and grown in Dulbecco's modified Eagle's medium (DMEM) (Invitrogen) supplemented with 100 U/ml penicillin/G-streptomycin (P/S), 10% heat inactivated fetal bovine serum (FBS) and Glutamax. Mouse 3T3-Swiss albino fibroblasts were obtained from ATCC (clone CCL-92) and cultured in DMEM, 10% calf bovine serum (CBS), and 1% P/S. Mouse C2C12 myoblasts were cultured in DMEM/Glutamax, 20% FBS and 1% P/S. All cell cultures were grown at 37 °C in a 5% CO_2 humidified chamber.

For the RNAi experiments, 1×10^5 cells were plated in DMEM medium with 5% FBS/CBS and without antibiotics, on 6-well plates. Approximately 1–2 h later, cells were transfected with 250 ng of siRNA–lipofectamine complexes prepared in Opti-MEM I medium (Invitrogen), according to manufacturer's instructions. Transfections with control siRNA (UBXD8) or with lipofectamine only (mock) were used as experimental controls.

For the overexpression experiments, 2 μg of pEGFP or pEGFP-ATXN3_28Q (kindly provided by Dr. H. Paulson) were used for each 6-well plate. Plasmid–lipofectamine complexes were transfected into HeLa cells and analyzed 48 h later.

For immunofluorescence procedure, cells were plated on 6-well plates containing poly-L-lysine coated glass coverslips.

2.3. Immunofluorescence

Depending on the antibodies, cells were fixed for 12 minutes (min) in freshly prepared 2% paraformaldehyde or fixed for 2 min in methanol/2 mM EGTA at −20 °C. Cells were then permeabilized with 0.5% Triton X-100 in PBS for 5 min or with 0.2% Triton X-100 in TBS for 7 min, respectively. Next, cells were blocked with 10% FBS for 30 min and then incubated with primary antibodies against ATXN3 (rabbit serum kindly provided by Dr. H. L. Paulson, 1:5000 dilution), anti-α-tubulin (1:100, DSHB, University of Iowa), anti-acetylated α-tubulin (1:2000, Sigma), anti-vimentin (1:1000, DSHB), anti-ubiquitin FK2 (1:5000, Biomol), anti-talin (1:200, SantaCruz Biotechnology). Alexa Fluor 488 and 568 conjugated secondary antibodies were used at 1:1500 (Molecular Probes). DNA was stained with DAPI (Sigma).

2.4. Microscopy analysis

Images were acquired as Z-stacks with 0.2–0.3 μm spacing using an Olympus FluoView FV1000 confocal microscope. Maximal intensity projections of the entire Z-stack are shown.

2.5. Real-time quantitative PCR (qPCR)

One microgram of total RNA purified from cells was reverse transcribed using the SuperScript kit (Invitrogen). The qPCR reaction was performed using the QuantiTec SYBR Green kit (Qiagen) and the primers described below in a LightCycler device (Roche). Primers used to amplify hATXN3, UBXD8 and HPRT were: MJD119F + MJD360R, UBXD8F + UBXD8R and HPRTF + HPRTR (Sup. Table 1). ATXN3 expression was normalized to HPRT levels within the sample. The normalized values of siATXN3 were then compared to controls using the ΔΔCt method [26]. Results are presented as fold change differences of siATNX3 relative to controls.

2.6. Immunoblotting

For cellular extracts, 40 μg of total protein isolated in NP-40 lysis buffer (150 mM NaCl, 50 mM Tris–HCl pH 7.6, 0.5% NP-40, 1 mM PMSF, Complete protease inhibitors (Roche)) were resolved in 10% SDS-Page gels and then transferred to a nitrocellulose membrane. The primary antibodies were incubated overnight at 4 °C: anti-MJD1.1 1:2000 [5], anti-α-tubulin (1:100, DSHB), anti-actin (1:2000, DSHB), anti-acetylated tubulin (1:2000, Sigma), anti-vimentin (1:500, DSHB), anti-talin (1:200, SantaCruz). After incubation with the secondary antibodies, membranes were incubated with the SuperSignal Chemiluminescence Substrate (Pierce). Films were then analyzed using ImageJ software.

2.7. α-integrin colorimetric array

Cells were grown and transfected as described above. To perform the array, ~2×10^6 cells/ml of each biological replicate were detached with PBS/3 mM EDTA with the help of a cell scrapper. After 3 washes

with PBS/3 mM EDTA to remove dead cells and clumps, cells were resuspended in assay buffer (provided with the kit); 100 μl of this suspension was plated into each well of the α- integrin-mediated cell adhesion array (ECM530, Chemicon) and incubated for 2 h at 37 °C in a 5% CO_2 humidifier chamber. Unbound cells were washed and after adding cell stain solution and extraction buffer as recommended by the protocol; absorbance was determined at 540 nm.

2.8. Cell cycle analysis

Cells transfected with control siRNA or siATXN3 were immunostained for phospho-H3 (Sigma) and α-tubulin in order to distinguish specific mitotic stages.

For flow cytometry analysis, 1×10^6 cells were trypsinized, collected in a 15 ml tube and washed several times with PBS. Cells were fixed using ice-cold 70% ethanol for 1 h in ice. Cells were washed with PBS to remove ethanol and then stained with propidium iodide solution (1 mg/ml propidium iodide, 800 μg/ml RNase in PBS) for 1 h at room temperature. Samples were washed with PBS and run into an EPICS XL-MCL flow cytometer (Beckman-Coulter Corporation) as described before [27]. A minimum of 30,000 cells per sample were acquired and an acquisition protocol was defined to measure forward scatter and red fluorescence on a linear scale. Data were analyzed using the Windows Multiple Document Interface for Flow Cytometry 2.8 (WinMDI 2.8). Four independent replicates were used for statistical analysis.

2.9. TUNEL assay

For the TUNEL assay, siATXN3 and control siRNA transfected cells were fixed, permeabilized and stained as advised by the manufacturer (In Situ Cell Death Detection Kit, POD, Roche). Cells were observed under a microscope and random fields were captured. TUNEL-positive cells were counted in each field and total number of cells was determined by DAPI positive staining.

2.10. MTS assay

Cells were plated onto 48-well plates and transfected with control siRNA or siATXN3. MTS reagent (CellTiter 96 Aqueous One Solution Assay, Promega) was added to each well according to manufacturer's instructions. After 4 h incubation, absorbance at 490 nm was read using a BioRad plate reader (BioRad).

2.11. Statistical analysis

For immunoblottings, the mean density and area of each band was measured using at least three independent experiments in ImageJ software. Comparison between control siRNA and siATXN3 groups was done using t-test in the SPSS version 16 software. For Real-Time PCR data, the same approach was used and results were presented using the ΔΔ Ct method.

3. Results

3.1. ATXN3 depletion leads to the formation of cellular ubiquitylated foci and morphological changes

In order to study the cellular role of ATXN3, we performed RNAi-mediated gene silencing with a pool of siRNAs specific against the human and mouse ATXN3 mRNAs. Transfection of siRNAs against ATXN3 into HeLa and C2C12 cells resulted in a significant reduction of both mRNA and protein levels (Fig. 1A, B, Sup. Fig. 1). The highest depletion levels of ATXN3 in HeLa and C2C12 cells occurred at 72 h and 48 h post-transfection, respectively, and the protein levels started to be restored after that period. Even though we have obtained efficient depletion of ATXN3 as determined by western blot using MJD1-1 antibody [5], the immunofluorescence signal for ATXN3 in the silenced cells was still visible, although lower than controls, especially in the nucleus (Fig. 1C, D). This is due to the fact that different antibodies were used for immunofluorescence and wb, since our antibody works poorly in immunofluorescence and the other recognized several additional bands in the wb. Therefore, the residual immunostaining in the immunofluorescence can correspond either to a different ATXN3 isoform or to unspecific proteins.

To further confirm the effectiveness of the siRNA, and since ATXN3 has DUB enzymatic activity, we checked ubiquitin immunoreactivity in siATXN3 transfected cells. As shown in Fig. 1C, the appearance of ubiquitylated foci was more frequently observed in siATXN3 than in control cells, although not all the siATXN3 cells displayed these foci. Incubation with the proteasomal inhibitor MG132 for 1 h further enhanced the formation of these foci in the siATXN3-treated cells (Fig. 1D). Interestingly, we observed that siATXN3 cells displayed an odd morphology when compared to control RNAi-transfected cells (Fig. 1C, D). In contrast with the stretched elliptical shape of controls, the shape of siATXN3-transfected cells was rounder with extensive loss of adhesion into the coverslip surface. Similar results were obtained for mouse C2C12 cells with reduced levels of ATX3 (data not shown).

3.2. ATXN3-depleted cells exhibit cytoskeletal defects

To test if the altered cellular morphology could be a consequence of cytoskeletal defects, we performed immunofluorescence analysis for the main components of the cytoskeleton: microtubules (α-tubulin), microfilaments (actin) and intermediate filaments (vimentin) in siATXN3-transfected cells.

As depicted in Fig. 2A, staining for α-tubulin revealed that the microtubule network was severely affected in siATXN3 cells in terms of the spatial array of the filaments: microtubules were randomly distributed in these cells in comparison to the parallel regular distribution observed in control cells. Microtubule nucleation from the MTOC/centrosome did not seem to be compromised in siATXN3 cells, and actually, there was an accumulation of filaments near this area in comparison with control cells (Fig. 2A). Considering that α-tubulin acetylation enhances microtubule stability [28] and that ATXN3 interacts with HDAC6, the protein that deacetylates α-tubulin [29], we thought it would be important to verify the levels and distribution of acetylated α-tubulin in siATXN3-transfected cells. Immunofluorescence assays revealed no apparent alteration in the levels of acetylated α-tubulin, besides the previously observed loss of parallel spreading of microtubules across the longest cell axis, suggesting that the microtubule stability is not compromised (Sup. Fig. 2).

As anticipated, staining of filamentous actin polymers with phalloidin in control cells showed the presence of parallel stress fibers and less prominent cortical actin, whereas siATXN3 cells displayed unparallel stress fibers with no significant differences in cortical actin (Fig. 2B). Analogous results were observed in mouse siATX3 transfected cells (Sup. Fig. 3).

The intermediate filaments were also irregularly distributed in ATXN3 silenced cells (Fig. 2C), exhibiting random spreading instead of the parallel scattering in control cells.

Although there was an overall disorganization of the cytoskeleton components in terms of spatial arrangement, their polymerization seemed to be unaffected (Fig 2).

The protein levels of α-tubulin, acetylated α-tubulin, actin and vimentin were similar in siATXN3 and control HeLa cells, as ascertained by western blot (Fig. 2D). Even though the levels of intact vimentin remained constant, we observed extra bands of lower molecular weight recognized by the antibody in the ATXN3-depleted cells, which might correspond to cleavage products arising from vimentin cleavage by caspases [30].

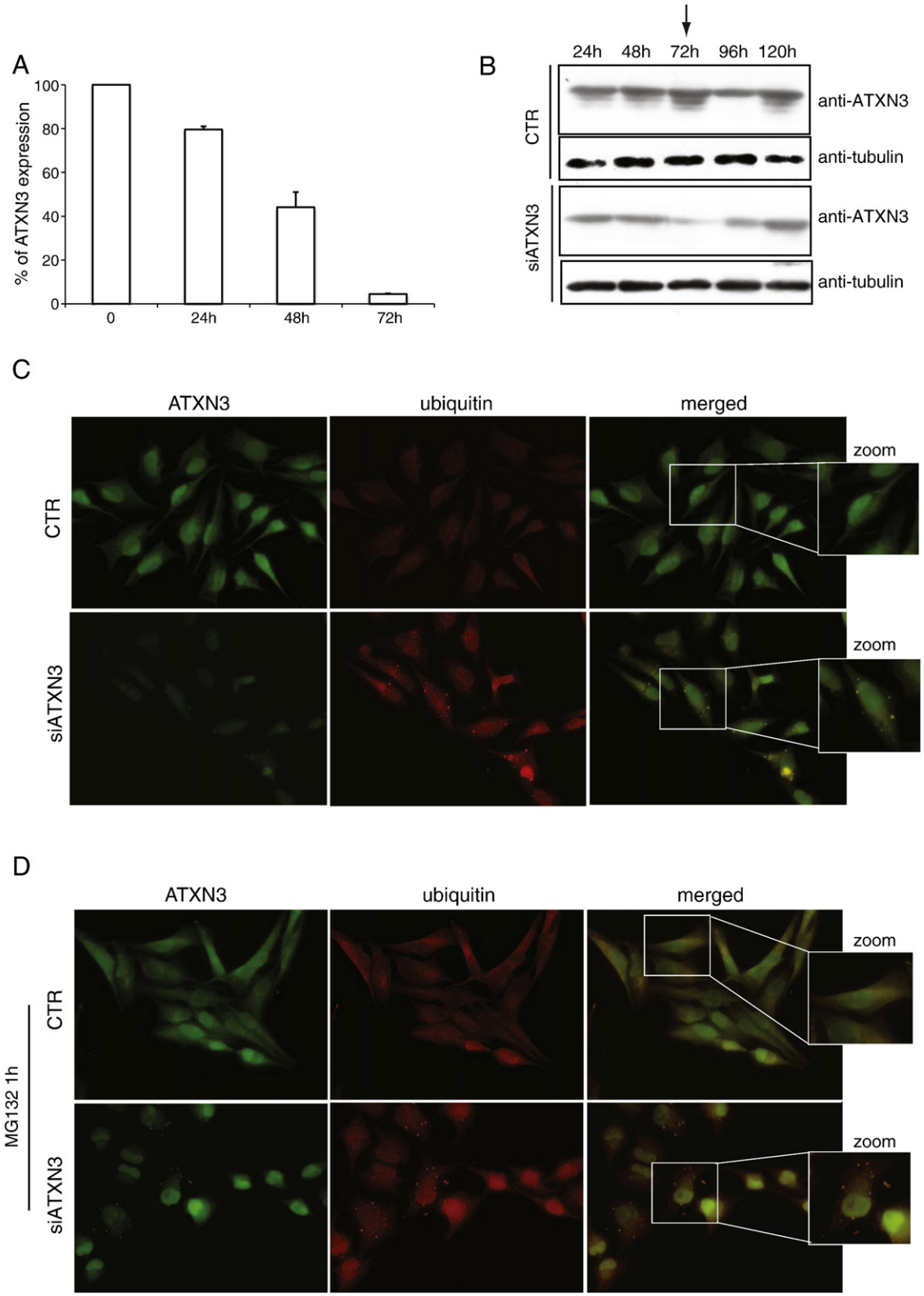

Fig. 1. ATXN3 depletion leads to ubiquitin-positive foci formation. Delivery of a pool of siRNAs against human ATXN3 lead to a significant reduction of its mRNA (A) and protein (B) levels in HeLa cells. (A) Quantitative RT-PCR results showing that ATXN3 levels were reduced during timecourse of RNAi reaching the maximum silencing at 72 h post-transfection. Shown is the graph of % of ATXN3 silencing in siATXN3-cells when compared to control RNAi cells. (B) Western blot showing that ATXN3 protein levels were also reduced at 72 h post-transfection and started to return to normal after 72 h, reaching normal levels at 120 h. α-tubulin was used as a loading control. (C) siATXN3 transfection leads to a slight increase in ubiquitin staining and the appearance of ubiquitylated foci in HeLa cells. This phenotype was further enhanced by administration of the proteasome inhibitor MG132. The siATXN3 cells were rounder when compared to the control cells. Scale bar: 20 μm. Rabbit anti-ATXN3 kindly provided by Dr. H. Paulson and stained with secondary antibody Alexa Fluor 468. Mouse anti-ubiquitin FK2 (Biomol), secondary antibody Alexa Fluor 568.

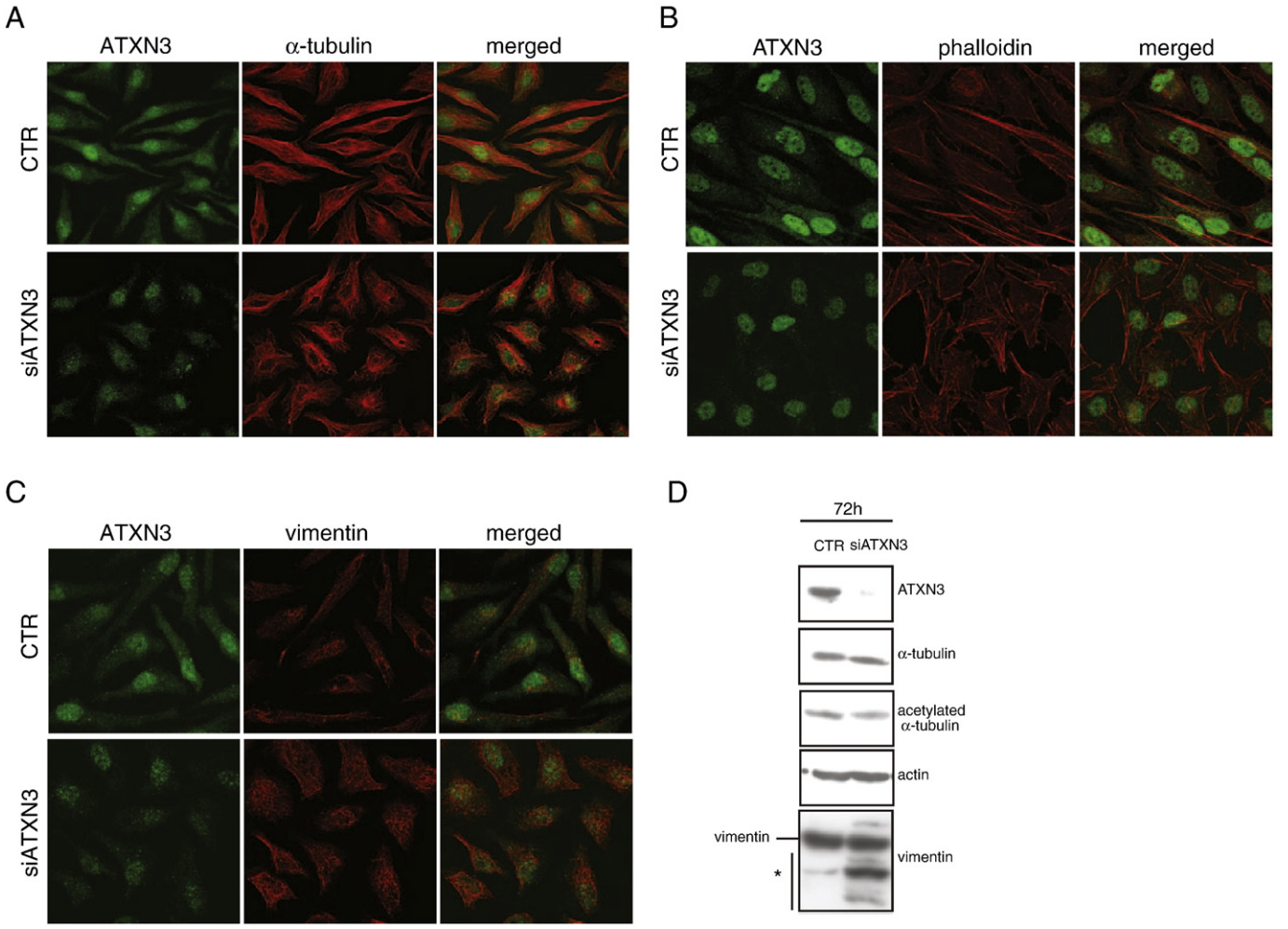

Fig. 2. ATXN3 depletion affects the cytoskeleton networks in HeLa cells. (A) Microtubules were disorganized and not parallel as in control cells. Microtubule nucleation from the MTOC/centrosome did not seem to be compromised in siATXN3 HeLa cells, instead there was an accumulation of filaments near the MTOC in comparison with control cells (arrows). (B) Actin filaments (stained with phalloidin) were unparallel in siATXN3 cells. (C) Vimentin exhibited random spreading when ATXN3 was depleted. (D) Western blot analysis of these cytoskeletal components shows that their levels were not affected in siATXN3 cells. Vimentin blot presented lower molecular weight bands (*), which can be putative proteolytic fragments, although the level of intact vimentin remained unchanged. Scale bar: 20 μm. Rabbit anti-ATXN3 kindly provided by Dr. H. Paulson and stained with secondary antibody Alexa Fluor 468. Mouse anti-tubulin and anti-vimentin from DSHB, secondary antibody Alexa Fluor 568. Phalloidin red from Molecular Probes.

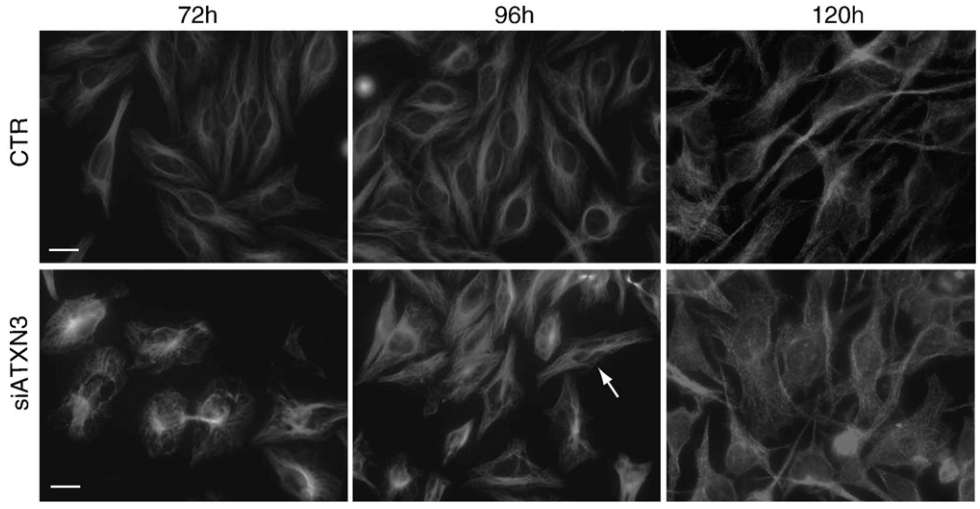

Fig. 3. The cytoskeletal phenotype observed in siATXN3 cells is dependent on ATXN3 levels. At 72 h post-transfection (lowest levels of ataxin-3), the phenotype of HeLa siATXN3-treated cells was evident: cells were rounder and the microtubule network was disorganized. At 96 h post-transfection, a timepoint when ataxin-3 levels were almost normal, cells still displayed a cytoskeletal-phenotype but many cells appeared as control cells (arrow). At 120 h post-transfection, when the levels of ATXN3 were normal, the cells no longer presented detectable microtubule disorganization, although a few cells were still rounder than controls. Immunofluorescence against a-tubulin using secondary antibody Alexa Fluor 568. Scale bar:20 μm.

3.3. Restoring ATXN3 levels ameliorates the phenotype of siATXN3 cells

In order to see if the RNAi-induced phenotype could be reverted once ATXN3 levels returned to normal, we examined cells 72, 96 and 120 h post-transfection with siATXN3, 120 h being the time point when ATXN3 protein was at normal levels. We found that the cellular morphology and microtubule organization was restored once ATXN3 protein levels returned to normal (Fig. 3). Therefore, we can conclude that the phenotype observed is reversible and dependent on ATXN3 levels.

3.4. ATXN3 RNAi leads to reduced focal adhesion formation and lower levels of α-1 integrin subunit at cell surface

Since we clearly observed an abnormal cell morphology in ATXN3 RNAi, we decided to analyze if the siATXN3-depleted cells also presented adhesion problems. Therefore, we investigated the focal adhesion points (FAs) through immunostaining for talin, a protein highly concentrated in regions of cell–substratum contact including FAs [31]. As shown in Fig. 4A, the talin expression pattern is altered in siATXN3 cells compared to controls, with significant loss of talin accumulation at FAs. Western blot analysis further confirmed the reduction of talin expression (Fig. 4B). Overexpression of wild type ATXN3 did not lead to any statistical differences in talin expression levels (Fig. 4B).

Since the connection between FAs and proteins of the extracellular matrix (ECM) generally involves integrins, and given that talin links integrins to the actin cytoskeleton [32], we also assessed the levels of integrin subunits in HeLa ATXN3-depleted cells. Using a colorimetric array that allows quantification of integrin expression at the cell surface with the use of specific antibodies, we observed that α1 integrin subunit was significantly less expressed in siATXN3 compared to control cells. The other α-integrin subunits did not change significantly, although α3, α5 and αV showed a tendency to be diminished (Fig. 4C).

3.5. ATXN3 knockdown leads to enhanced cell death in the absence of mitotic index alterations

Our next aim was to determine which were the consequences of the cytoskeletal and adhesion problems in ATXN3-depleted cells. Given that a correct cell division requires an intact microtubule network and the fact that ATXN3 interacts with α-tubulin and binds microtubules in human, mouse and *C. elegans*, with a peculiar distribution during cell cycle (Sup. Fig. 4), we asked if the cell cycle progression could be altered in siATXN3-depleted cells. To appraise

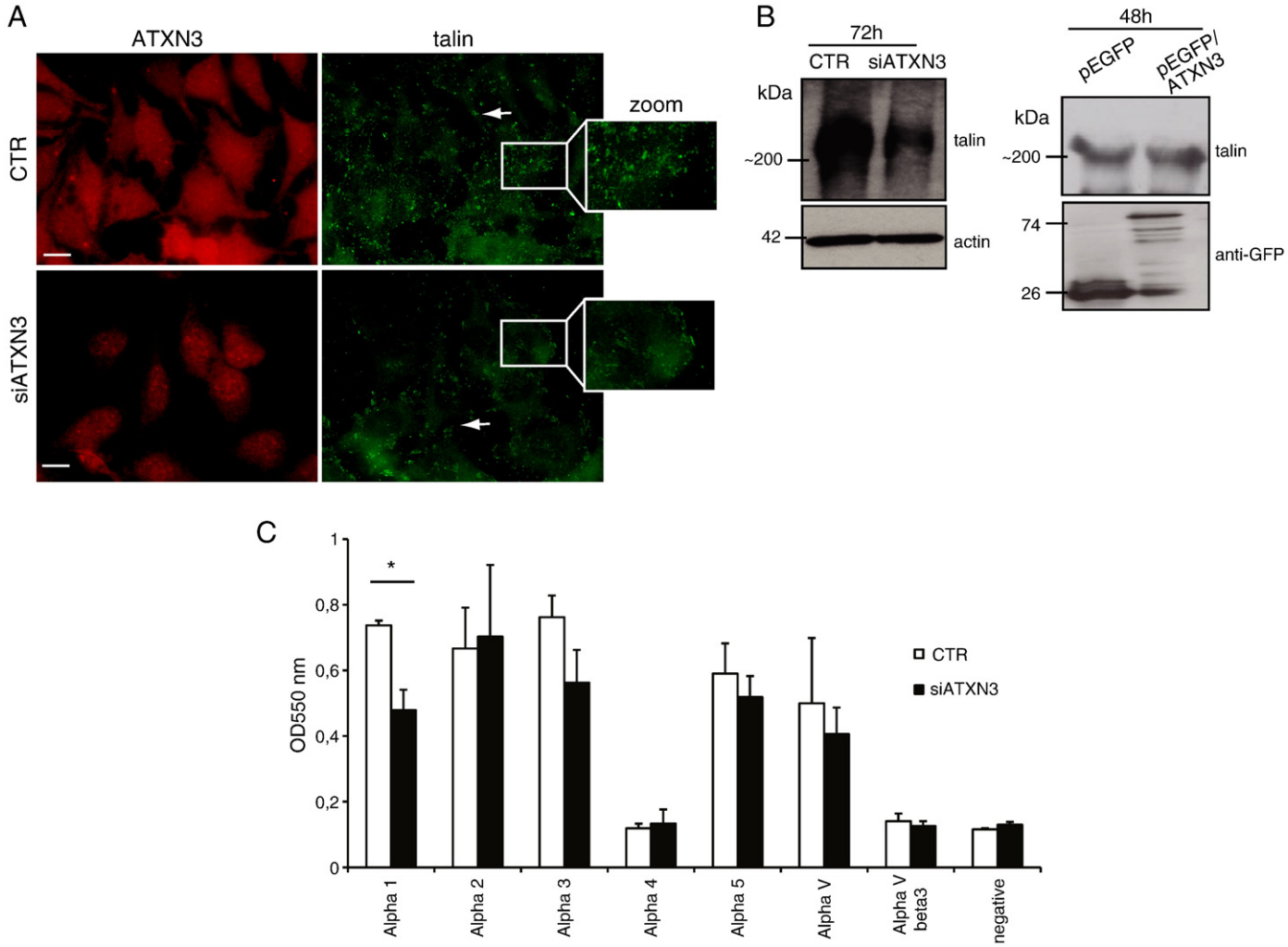

Fig. 4. ATXN3 RNAi causes a decrease of cell adhesion molecules. Talin expression was decreased in ATXN3-depleted cells as ascertained by immunofluorescence (A) and western blot (B). (C) siATXN3 cells expressed lower levels of α1 integrin subunit at their surface (*t*-test, $^*p<0.05$) as measured using the Alpha Integrin-Mediated Cell Adhesion Array. Integrin subunit α4 and αVβ3 integrin were not expressed in HeLa cells. Negative control refers to wells coated with BSA. Error bars refer to standard deviation of 3 independent biological replicates. Scale bar: 10 μm. Rabbit anti-ATXN3 kindly provided by Dr. H. Paulson and stained with secondary antibody Alexa Fluor 568. Goat anti-talin from SantaCruz Biotechnology, secondary antibody Alexa Fluor 488.

this, we determined the mitotic index of a cell population by counting the number of cells immunopositive for phosphorylated histone H3 over the total number of cells [33] and evaluated the cellular DNA content using propidium iodide staining and flow cytometry analysis [34]. As illustrated in Fig. 5A, the mitotic index was similar in control and siATXN3 knockdown cells (72 h after transfection) and there was no accumulation of mitotic cells in any specific stage compared to controls (Fig. 5B). Flow cytometry analysis revealed that siATXN3-treated cells were cycling similarly to control cells, except that there was an increase in the sub-G0/G1 population, 13.2% compared to 7.0% of control cells, consistent with the appearance of a sub-population with a decreased forward scatter highly correlated with a decrease in cell size (Fig. 5C). In addition, MTS assays revealed that siATXN3-depleted cells had reduced metabolic activity (Fig. 5D). Considering

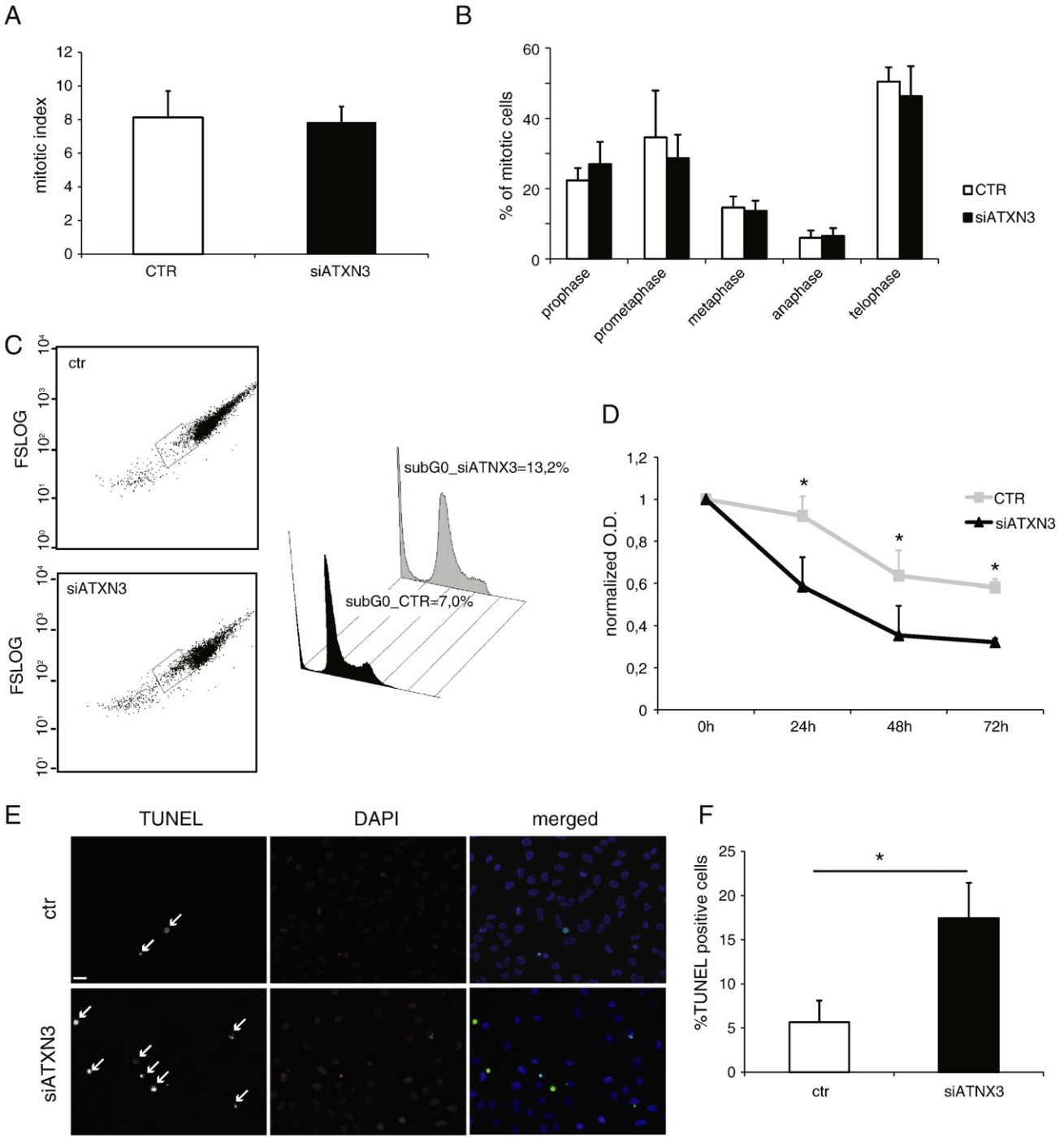

Fig. 5. ATXN3 depletion does not impair the mitotic cycle but increases cell death in HeLa cells. (A) Mitotic index was similar between control and ATXN3-depleted cells as ascertained by mitotic cell counting using phospho-H3 and α-tubulin immunostaining. (B) The distribution of siATXN3 cells throughout the mitotic stages was similar to control (CTR). (C) Flow cytometry (FCM) analysis showed an increase in cell population with abnormal size (forward scatter—FSLOG) in siATXN3 cells when compared to control RNAi (population inside square). An increase in sub-G0/G1 population was observed using propidium iodide staining followed by FCM analysis: Ctr = 7 ± 1.1%, siATXN3 = 13.2 ± 1.0% (*t*-test, $^*p<0.05$). (D) MTS assay revealed that siATXN3-transfected cells displayed lower metabolic activity than that of controls from 24 h until 72 h post-transfection (*t*-test, $^*p<0.05$). (E, F) TUNEL assay confirming that ATXN3 depletion lead to an increase in cell death. A 20× magnification random field of cells from a representative experiment is shown (E). Controls presented some cell death although to a less extent than siATXN3 cells: Ctr = 5.6%, siATNX3 = 17.4% (F). Error bars refer to standard deviation. $n \geq 3$ independent biological replicates in all experiments. Scale bar: 20 μm.

that an increase in sub-G0/G1 population and a decrease in metabolic activity are good indicators of cellular death, and the fact that cytoskeletal defects and adhesion problems are frequently accompanied by an increase in cell death, a mechanism known as anoikis [35], we used the TUNEL assay to determine the occurrence of DNA fragmentation-associated cell death. SiATXN3 cells revealed an increased TUNEL staining (17.4%), indicative of cell death, when compared to control RNAi (5.6%) (Fig. 5E, F). Thus, data indicate that ATXN3 knockdown leads to enhanced cell death in the absence of significant mitotic index alterations.

4. Discussion

In polyQ diseases such as MJD, although the polyQ tract itself is thought to be pathogenic, partial loss of the normal function of the proteins might contribute for the overall pathology and be responsible for disease-specific features [1,36,37]. For example, the differential neuronal vulnerability observed in each polyQ disease may be explained by the distinct protein context or protein interactions of the specific protein involved in that disease. Since the cloning of the *ATXN3* gene in 1994, several efforts have been made to understand its biochemical function, however, the exact biological role of ATXN3 remains undisclosed.

Here, we report a cellular phenotype due to the absence of ATXN3, i.e., cells accumulate ubiquitylated foci, display cytoskeletal and adhesion defects and increased cell death. Analogous to the mouse ATXN3 knockout model, which also accumulates ubiquitylated proteins [38], our cellular model of ATXN3 deficiency presented ubiquitin-positive foci, a signal of cellular stress. As expected, the formation of foci was augmented by the addition of the proteasomal inhibitor MG132. These foci are not aggresomes, as they are smaller structures and do not accumulate near the MTOC area. This finding is in agreement with other studies which show that ATXN3 depletion inhibits aggresome formation even in stressful situations [22]. It has been suggested that ATXN3 DUB activity is required for the formation of aggresomes, as it may stabilize proteins involved in the trafficking of misfolded proteins [22]. In addition, we hypothesize that ATXN3 absence leads to cytoskeletal defects, especially in the microtubule network, which may contribute to the inability to form aggresomes, a microtubule-dependent process [19,39].

The formation of ubiquitylated foci may suggest that ATXN3 can act as a DUB *in vivo*, and imply that the proteins accumulating in these foci may be putative substrates of ATXN3 DUB activity. While some studies suggest that the expansion does not affect ATXN3 DUB activity, at least *in vitro* [3,10], others suggest that it does [2,8]. For instance, ERAD substrates have been shown to accumulate in the presence of expanded ATXN3 [8], suggesting that the mutant protein may loose some of its activity leading to substrate accumulation. Hence, it is very appealing to assess what is the protein constitution of these ubiquitylated foci accumulating in siATXN3 cells, in order to identify potential ATXN3 substrates, which may eventually be interesting therapeutic targets.

In this work, in addition to the *canonical* role proposed for ATXN3 in the UPP, we also found that ATXN3 may have a role in cytoskeleton organization. Cells with reduced levels of ATXN3 present clear morphological changes; they are rounder and display less projections. The polymerization of the microtubule network does not seem to be affected, but this network is disorganized, with filaments distributed in a random rather than parallel fashion, which was a quite interesting finding if we consider the physical interaction of ATXN3 with α-tubulin and its ability to bind to microtubules. Dynein is a motor protein recruited to sites of cell–cell contact, co-localizing with β-catenin, where it is thought to tether and stabilize the microtubules. Overexpression of β-catenin and subsequent alteration of dynein cellular localization severely affects the microtubule array organization [40]. Since ATXN3 is known to interact with dynein [22], if dynein localization/function is somehow perturbed in the absence of ATXN3, this could originate the microtubule disorganization.

The microfilament and intermediate filament networks were also affected in siATXN3-treated cells. This is not so surprising as it is known that disruption of one of the cytoskeletal components also affects the others. For example, several drugs that disrupt or redistribute microtubules, such as taxol, also affect the intermediate filaments [41]. One can hypothesize that the absence of ATXN3 can first lead to the microtubule disorganization, that in turns affects the organization of other cytoskeletal components.

It is unlikely, however, that the major cytoskeletal proteins are direct substrates of ATXN3 DUB activity, as their levels remained the same in siATXN3 cells. Nevertheless, we cannot exclude the possibility that ATXN3 may be modulating the degradation of other proteins important for a correct cytoskeletal organization.

In addition to the cytoskeletal defects, we detected a decrease in the expression of important adhesion-related molecules such as talin and α1 integrin subunit, indicating that the ECM–cell or cell–cell interconnection was compromised. Integrins are receptors that are responsible for binding to specific ECM proteins and other cells [42]. Concordantly, in a parallel study, we have observed that reduction of mATXN3 in C2C12 differentiating cells leads to a decrease of α-5 and α-7 integrin subunits and talin expression among other proteins important for adhesion, and causes a muscle differentiation delay (MC Costa et al, unpublished observations). Talin is a ubiquitous protein highly expressed in focal adhesions (FAs) that links integrins to the actin network [42]. Although we found a significant downregulation of talin protein in siATXN3-treated cells, overexpression of wild type ATXN3 did not lead to any differences in talin expression levels when compared to control cells. Considering the putative role of ATXN3 in the protein degradation pathway, this finding may indicate that talin is not a substrate of ATXN3 and its downregulation may be an indirect effect of ATXN3 depletion and consequent cytoskeletal abnormalities, which we did not observe in ATXN3-overexpressing cells (data not shown). Nevertheless, we can also consider that even if ATXN3 is being overexpressed, if other proteins important for talin degradation are present in normal levels, the talin levels may remain the same in both control and ATXN3-overexpressing cells.

The abnormal cytoskeleton, especially the microtubule disorganization, can explain the morphological changes of siATXN3 cells, as it is known that the microtubules can mediate cell shape through interactions with the actin network in the focal adhesions (FAs) [43]. Furthermore, some studies that have shown that microtubule disruption perturbs FA organization, and causes de-regulation of integrin expression at the cell membrane [44], which we also observe. However, we cannot exclude the possibility that changes in integrin levels might be the upstream cause of the cytoskeletal phenotype of ATXN3-depleted cells.

Given that the cytoskeleton, in particular the microtubules, plays a fundamental role during mitosis, we analyzed the cell cycle progression in ATXN3-depleted cells. We did not find any differences in mitotic index and mitotic stage distribution. However, an increase in sub-G0/G1 population was observed in siATXN3-transfected cells, indicative of cell death, which was indeed confirmed by the TUNEL assay. It is unlikely that cell death occurs due to mitotic abnormalities but rather due to the morphological changes observed. It has been proven that conditions affecting microtubules lead to cytoskeleton defects and adhesion problems that are later accompanied by cell rounding, cell detachment and consequently cell death-anoikis [44,45], a similar phenotype as the one we observe for siATXN3-treated cells. Another interesting finding is the appearance of several vimentin-immunoreactive low molecular weight bands in siATXN3-transfected cells. Vimentin is known to be degraded by caspases in response to apoptotic inducers, probably to facilitate nuclear condensation and fragmentation. Moreover, vimentin cleavage also generates an amino-terminal fragment which induces apoptosis, a

process dependent on caspase activity [31]. We can hypothesize that, in the case of siATXN3-transfected cells, vimentin is being degraded to facilitate nuclear fragmentation and apoptosis of cells with abnormal morphology and/or that its cleavage is inducing apoptosis.

One intriguing aspect of this work is the apparent discrepancy in the phenotype of the available ATXN3 knockout animals and the cellular model of ATXN3 deficiency we report here. While the *C. elegans* ataxin-3 knockout animals are apparently normal [24], the knockout mouse model only shows a mild increase in ubiquitylation levels [38]. Cells with reduced ATXN3 levels accumulate ubiquitylated foci, display cytoskeletal and adhesion problems and increased cell death. Although the presence of ubiquitylated foci in siATXN3 cells can parallel the increase in ubiquitin levels in the mouse knockout model, the cytoskeletal and adhesion deficits were never detected before. Nevertheless, it has been shown that compensation and adaptative mechanisms can occur in organisms due to the long-term absence of a certain protein and some phenotypes only arise in specific cell types and not in the whole organism. For example, the vimentin knockout mice are viable and without any obvious phenotype [46] while their cultured fibroblasts have abnormal mechanical properties and are significantly more fragile [47]. We also cannot exclude the fact that very subtle cytoskeletal defects may exist in these ATXN3 knockout models, which were undetectable using a gross phenotypical analysis. For example, although apparently normal in a basal situation, the *C. elegans* ataxin-3 knockout animals display a severe motility defect at a stress-threshold growth condition [48]. Furthermore, recent work from R. Pittman lab has shown that the fibroblasts from ATXN3 knockout mice are more sensitive to heat stress than fibroblasts from wild type [49]. Together, these findings indicate that additional studies have to be performed in the available knockout models in order to ascertain how “normal” they really are.

Our work associates ATXN3 with cytoskeletal organization raising the possibility that a partial loss of function of this protein can also be relevant in the disease context by affecting the neuronal cytoskeleton network.

Acknowledgments

Authors would like to thank Agostinho Almeida for the help in the flow cytometry and Paula Ludovico for critical comments on the manuscript. AJR and MCC would like to thank all members of the PM lab for helpful discussions. This work was financed by the Fundação para a Ciência e a Tecnologia (FCT) (POCI/SAU-MMO/60412/2004). AJR, MCC and TS were supported by the FCT fellowships SFRH/BD/17066/2004, SFRH/BD/9759/2003 and SFRH/BI/33504/2008, respectively.

Appendix A. Supplementary Data

Supplementary data associated with this article can be found, in the online version, at doi:10.1016/j.bbamcr.2010.07.004.

References

[1] A.R. La Spada, J.P. Taylor, Polyglutamines placed into context, Neuron 38 (2003) 681–684.
[2] E.W. Doss-Pepe, E.S. Stenroos, W.G. Johnson, K. Madura, Ataxin-3 interactions with rad23 and valosin-containing protein and its associations with ubiquitin chains and the proteasome are consistent with a role in ubiquitin-mediated proteolysis, Mol. Cell. Biol. 23 (2003) 6469–6483.
[3] B. Burnett, F. Li, R.N. Pittman, The polyglutamine neurodegenerative protein ataxin-3 binds polyubiquitylated proteins and has ubiquitin protease activity, Hum. Mol. Genet. 12 (2003) 3195–3205.
[4] Y. Chai, S.S. Berke, R.E. Cohen, H.L. Paulson, Poly-ubiquitin binding by the polyglutamine disease protein ataxin-3 links its normal function to protein surveillance pathways, J. Biol. Chem. 279 (2004) 3605–3611.
[5] A. Ferro, A.L. Carvalho, A. Teixeira-Castro, C. Almeida, R.J. Tome, L. Cortes, et al., NEDD8: a new ataxin-3 interactor, Biochim. Biophys. Acta 1773 (2007) 1619–1627.
[6] S.J. Berke, Y. Chai, G.L. Marrs, H. Wen, H.L. Paulson, Defining the role of ubiquitin-interacting motifs in the polyglutamine disease protein, ataxin-3, J. Biol. Chem. 280 (2005) 32026–32034.
[7] Y.C. Tsai, P.S. Fishman, N.V. Thakor, G.A. Oyler, Parkin facilitates the elimination of expanded polyglutamine proteins and leads to preservation of proteasome function, J. Biol. Chem. 278 (2003) 22044–22055.
[8] X. Zhong, R.N. Pittman, Ataxin-3 binds VCP/p97 and regulates retrotranslocation of ERAD substrates, Hum. Mol. Genet. 15 (2006) 2409–2420.
[9] Q. Wang, L. Li, Y. Ye, Regulation of retrotranslocation by p97-associated deubiquitinating enzyme ataxin-3, J. Cell Biol. 174 (2006) 963–971.
[10] B.J. Winborn, S.M. Travis, S.V. Todi, K.M. Scaglione, P. Xu, A.J. Williams, et al., The deubiquitinating enzyme ataxin-3, a polyglutamine disease protein, edits Lys63 linkages in mixed linkage ubiquitin chains, J. Biol. Chem. 283 (2008) 26436–26443.
[11] T. Woelk, S. Sigismund, L. Penengo, S. Polo, The ubiquitination code: a signalling problem, Cell Div. 2 (2007) 11.
[12] F. Li, T. Macfarlan, R.N. Pittman, D. Chakravarti, Ataxin-3 is a histone-binding protein with two independent transcriptional corepressor activities, J. Biol. Chem. 277 (2002) 45004–45012.
[13] B.O. Evert, J. Araujo, A.M. Vieira-Saecker, R.A. de Vos, S. Harendza, T. Klockgether, et al., Ataxin-3 represses transcription via chromatin binding, interaction with histone deacetylase 3, and histone deacetylation, J. Neurosci. 26 (2006) 11474–11486.
[14] C.T. McMurray, Neurodegeneration: diseases of the cytoskeleton? Cell Death Differ. 7 (2000) 861–865.
[15] S. Gunawardena, L.S. Goldstein, Polyglutamine diseases and transport problems: deadly traffic jams on neuronal highways, Arch. Neurol. 62 (2005) 46–51.
[16] A.C. Alonso, I. Grundke-Iqbal, K. Iqbal, Alzheimer's disease hyperphosphorylated tau sequesters normal tau into tangles of filaments and disassembles microtubules, Nat. Med. 2 (1996) 783–787.
[17] S. Engelender, A.H. Sharp, V. Colomer, M.K. Tokito, A. Lanahan, P. Worley, et al., Huntingtin-associated protein 1 (HAP1) interacts with the p150Glued subunit of dynactin, Hum. Mol. Genet. 6 (1997) 2205–2212.
[18] G. Hoffner, P. Kahlem, P. Djian, Perinuclear localization of huntingtin as a consequence of its binding to microtubules through an interaction with beta-tubulin: relevance to Huntington's disease, J. Cell Sci. 115 (2002) 941–948.
[19] J.A. Johnston, C.L. Ward, R.R. Kopito, Aggresomes: a cellular response to misfolded proteins, J. Cell Biol. 143 (1998) 1883–1898.
[20] Y. Kawaguchi, J.J. Kovacs, A. McLaurin, J.M. Vance, A. Ito, et al., The deacetylase HDAC6 regulates aggresome formation and cell viability in response to misfolded protein stress, Cell 115 (2003) 727–738.
[21] J.A. Johnston, M.E. Illing, R.R. Kopito, Cytoplasmic dynein/dynactin mediates the assembly of aggresomes, Cell Motil. Cytoskeleton 53 (2002) 26–38.
[22] B.G. Burnett, R.N. Pittman, The polyglutamine neurodegenerative protein ataxin 3 regulates aggresome formation, Proc. Natl. Acad. Sci. USA 102 (2005) 4330–4335.
[23] M.C. Costa, J. Gomes-da-Silva, C.J. Miranda, J. Sequeiros, M.M. Santos, P. Maciel, et al., Genomic structure, promoter activity, and developmental expression of the mouse homologue of the Machado–Joseph disease (MJD) gene, Genomics 84 (2004) 361–373.
[24] A.J. Rodrigues, G. Coppola, C. Santos, M.C. Costa, M. Ailion, J. Sequeiros, et al., Functional genomics and biochemical characterization of the C. elegans orthologue of the Machado–Joseph disease protein ataxin-3, FASEB J. 21 (2007) 1126–1136.
[25] S. Mazzucchelli, A. De Palma, M. Riva, A. D'Urzo, C. Pozzi, V. Pastori, et al., Proteomic and biochemical analyses unveil tight interaction of ataxin-3 with tubulin, Int. J. Biochem. Cell Biol. (2009).
[26] M.W. Pfaffl, A new mathematical model for relative quantification in real-time RT-PCR, Nucleic Acids Res. 29 (2001) e45.
[27] A.J. Almeida, D.R. Matute, J.A. Carmona, M. Martins, I. Torres, J.G. McEwen, et al., Genome size and ploidy of *Paracoccidioides brasiliensis* reveals a haploid DNA content: flow cytometry and GP43 sequence analysis, Fungal Genet. Biol. 44 (2007) 25–31.
[28] G. Piperno, M. LeDizet, X.J. Chang, Microtubules containing acetylated alpha-tubulin in mammalian cells in culture, J. Cell Biol. 104 (1987) 289–302.
[29] C. Hubbert, A. Guardiola, R. Shao, Y. Kawaguchi, A. Ito, A. Nixon, et al., HDAC6 is a microtubule-associated deacetylase, Nature 417 (2002) 455–458.
[30] Y. Byun, F. Chen, R. Chang, M. Trivedi, K.J. Green, V.L. Cryns, Caspase cleavage of vimentin disrupts intermediate filaments and promotes apoptosis, Cell Death Differ. 8 (2001) 443–450.
[31] K. Burridge, L. Connell, Talin: a cytoskeletal component concentrated in adhesion plaques and other sites of actin-membrane interaction, Cell Motil. 3 (1983) 405–417.
[32] D.R. Critchley, Focal adhesions—the cytoskeletal connection, Curr. Opin. Cell Biol. 12 (2000) 133–139.
[33] M.J. Hendzel, Y. Wei, M.A. Mancini, A. Van Hooser, T. Ranalli, B.R. Brinkley, et al., Mitosis-specific phosphorylation of histone H3 initiates primarily within pericentromeric heterochromatin during G2 and spreads in an ordered fashion coincident with mitotic chromosome condensation, Chromosoma 106 (1997) 348–360.
[34] A. Krishan, Rapid flow cytofluorometric analysis of mammalian cell cycle by propidium iodide staining, J. Cell Biol. 66 (1975) 188–193.
[35] S.M. Frisch, R.A. Screaton, Anoikis mechanisms, Curr. Opin. Cell Biol. 13 (2001) 555–562.
[36] E. Cattaneo, D. Rigamonti, D. Goffredo, C. Zuccato, F. Squitieri, S. Sipione, et al., Loss of normal huntingtin function: new developments in Huntington's disease research, Trends Neurosci. 24 (2001) 182–188.
[37] J. Lim, J. Crespo-Barreto, P. Jafar-Nejad, A.B. Bowman, R. Richman, et al., Opposing effects of polyglutamine expansion on native protein complexes contribute to SCA1, Nature 452 (2008) 713–718.

[38] I. Schmitt, M. Linden, H. Khazneh, B.O. Evert, P. Breuer, T. Klockgether, et al., Inactivation of the mouse Atxn3 (ataxin-3) gene increases protein ubiquitination, Biochem. Biophys. Res. Commun. 362 (2007) 734–739.
[39] R. Garcia-Mata, Z. Bebok, E.J. Sorscher, E.S. Sztul, Characterization and dynamics of aggresome formation by a cytosolic GFP-chimera, J. Cell Biol. 146 (1999) 1239–1254.
[40] L.A. Ligon, S. Karki, M. Tokito, E.L. Holzbaur, Dynein binds to beta-catenin and may tether microtubules at adherens junctions, Nat. Cell Biol. 3 (2001) 913–917.
[41] S. Forry-Schaudies, J.M. Murray, Y. Toyama, H. Holtzer, Effects of colcemid and taxol on microtubules and intermediate filaments in chick embryo fibroblasts, Cell Motil. Cytoskeleton 6 (1986) 324–338.
[42] D.A. Calderwood, S.J. Shattil, M.H. Ginsberg, Integrins and actin filaments: reciprocal regulation of cell adhesion and signaling, J. Biol. Chem. 275 (2000) 22607–22610.
[43] A.F. Palazzo, G.G. Gundersen, Microtubule-actin cross-talk at focal adhesions, Sci. STKE 2002 (2002) PE31.
[44] R.G. Deschesnes, A. Patenaude, J.L. Rousseau, J.S. Fortin, C. Ricard, M.F. Côté, et al., Microtubule-destabilizing agents induce focal adhesion structure disorganization and anoikis in cancer cells, J. Pharmacol. Exp. Ther. 320 (2007) 853–864.
[45] S.M. Frisch, H. Francis, Disruption of epithelial cell–matrix interactions induces apoptosis, J. Cell Biol. 124 (1994) 619–626.
[46] E. Colucci-Guyon, M.M. Portier, I. Dunia, D. Paulin, S. Pournin, C. Babinet, Mice lacking vimentin develop and reproduce without an obvious phenotype, Cell 79 (1994) 679–694.
[47] R.D. Goldman, S. Khuon, Y.H. Chou, P. Opal, P.M. Steinert, The function of intermediate filaments in cell shape and cytoskeletal integrity, J. Cell Biol. 134 (1996) 971–983.
[48] A.J. Rodrigues, A. Neves-Carvalho, A. Ferro, A. Rokka, G. Corthals, E. Logarinho, et al., ATX-3, CDC-48 and UBXN-5: a new trimolecular complex in Caenorhabditis elegans, Biochem. Biophys. Res. Commun. 386 (2009) 575–581.
[49] C.P. Reina, X. Zhong, R.N. Pittman, Proteotoxic stress increases nuclear localization of ataxin-3, Hum. Mol. Genet. (2009).